

Measurement of the Λ_b^0 Lifetime in $\Lambda_b^0 \rightarrow J/\psi \Lambda^0$ in $p\bar{p}$ Collisions at $\sqrt{s} = 1.96$ TeV

A. Abulencia,²³ J. Adelman,¹³ T. Affolder,¹⁰ T. Akimoto,⁵⁵ M.G. Albrow,¹⁶ D. Ambrose,¹⁶ S. Amerio,⁴³ D. Amidei,³⁴ A. Anastassov,⁵² K. Anikeev,¹⁶ A. Annovi,¹⁸ J. Antos,¹ M. Aoki,⁵⁵ G. Apollinari,¹⁶ J.-F. Arguin,³³ T. Arisawa,⁵⁷ A. Artikov,¹⁴ W. Ashmanskas,¹⁶ A. Attal,⁸ F. Azfar,⁴² P. Azzi-Bacchetta,⁴³ P. Azzurri,⁴⁶ N. Bacchetta,⁴³ W. Badgett,¹⁶ A. Barbaro-Galtieri,²⁸ V.E. Barnes,⁴⁸ B.A. Barnett,²⁴ S. Baroiant,⁷ V. Bartsch,³⁰ G. Bauer,³² F. Bedeschi,⁴⁶ S. Behari,²⁴ S. Belforte,⁵⁴ G. Bellettini,⁴⁶ J. Bellinger,⁵⁹ A. Belloni,³² D. Benjamin,¹⁵ A. Beretvas,¹⁶ J. Beringer,²⁸ T. Berry,²⁹ A. Bhatti,⁵⁰ M. Binkley,¹⁶ D. Bisello,⁴³ R.E. Blair,² C. Blocker,⁶ B. Blumenfeld,²⁴ A. Bocci,¹⁵ A. Bodek,⁴⁹ V. Boisvert,⁴⁹ G. Bolla,⁴⁸ A. Bolshov,³² D. Bortoletto,⁴⁸ J. Boudreau,⁴⁷ A. Boveia,¹⁰ B. Brau,¹⁰ L. Brigliadori,⁵ C. Bromberg,³⁵ E. Brubaker,¹³ J. Budagov,¹⁴ H.S. Budd,⁴⁹ S. Budd,²³ S. Budroni,⁴⁶ K. Burkett,¹⁶ G. Busetto,⁴³ P. Bussey,²⁰ K. L. Byrum,² S. Cabrera,¹⁵ M. Campanelli,¹⁹ M. Campbell,³⁴ F. Canelli,¹⁶ A. Canepa,⁴⁸ S. Carrillo,¹⁷ D. Carlsmith,⁵⁹ R. Carosi,⁴⁶ S. Carron,³³ M. Casarsa,⁵⁴ A. Castro,⁵ P. Catastini,⁴⁶ D. Cauz,⁵⁴ M. Cavalli-Sforza,³ A. Cerri,²⁸ L. Cerrito,³⁰ S.H. Chang,²⁷ Y.C. Chen,¹ M. Chertok,⁷ G. Chiarelli,⁴⁶ G. Chlachidze,¹⁴ F. Chlebana,¹⁶ I. Cho,²⁷ K. Cho,²⁷ D. Chokheli,¹⁴ J.P. Chou,²¹ G. Choudalakis,³² S.H. Chuang,⁵⁹ K. Chung,¹² W.H. Chung,⁵⁹ Y.S. Chung,⁴⁹ M. Ciljak,⁴⁶ C.I. Ciobanu,²³ M.A. Ciocci,⁴⁶ A. Clark,¹⁹ D. Clark,⁶ M. Coca,¹⁵ G. Compostella,⁴³ M.E. Convery,⁵⁰ J. Conway,⁷ B. Cooper,³⁵ K. Copic,³⁴ M. Cordelli,¹⁸ G. Cortiana,⁴³ F. Crescioli,⁴⁶ C. Cuenca Almenar,⁷ J. Cuevas,¹¹ R. Culbertson,¹⁶ J.C. Cully,³⁴ D. Cyr,⁵⁹ S. DaRonco,⁴³ S. D'Auria,²⁰ T. Davies,²⁰ M. D'Onofrio,³ D. Dagenhart,⁶ P. de Barbaro,⁴⁹ S. De Cecco,⁵¹ A. Deisher,²⁸ G. De Lentdecker,⁴⁹ M. Dell'Orso,⁴⁶ F. Delli Paoli,⁴³ L. Demortier,⁵⁰ J. Deng,¹⁵ M. Deninno,⁵ D. De Pedis,⁵¹ P.F. Derwent,¹⁶ C. Dionisi,⁵¹ B. Di Ruzza,⁵⁴ J.R. Dittmann,⁴ P. DiTuro,⁵² C. Dörr,²⁵ S. Donati,⁴⁶ M. Donega,¹⁹ P. Dong,⁸ J. Donini,⁴³ T. Dorigo,⁴³ S. Dube,⁵² J. Efron,³⁹ R. Erbacher,⁷ D. Errede,²³ S. Errede,²³ R. Eusebi,¹⁶ H.C. Fang,²⁸ S. Farrington,²⁹ I. Fedorko,⁴⁶ W.T. Fedorko,¹³ R.G. Feild,⁶⁰ M. Feindt,²⁵ J.P. Fernandez,³¹ R. Field,¹⁷ G. Flanagan,⁴⁸ A. Foland,²¹ S. Forrester,⁷ G.W. Foster,¹⁶ M. Franklin,²¹ J.C. Freeman,²⁸ I. Furic,¹³ M. Gallinaro,⁵⁰ J. Galyardt,¹² J.E. Garcia,⁴⁶ F. Garberson,¹⁰ A.F. Garfinkel,⁴⁸ C. Gay,⁶⁰ H. Gerberich,²³ D. Gerdes,³⁴ S. Giagu,⁵¹ P. Giannetti,⁴⁶ A. Gibson,²⁸ K. Gibson,⁴⁷ J.L. Gimmell,⁴⁹ C. Ginsburg,¹⁶ N. Giokaris,¹⁴ M. Giordani,⁵⁴ P. Giromini,¹⁸ M. Giunta,⁴⁶ G. Giurgiu,¹² V. Glagolev,¹⁴ D. Glenzinski,¹⁶ M. Gold,³⁷ N. Goldschmidt,¹⁷ J. Goldstein,⁴² G. Gomez,¹¹ G. Gomez-Ceballos,¹¹ M. Goncharov,⁵³ O. González,³¹ I. Gorelov,³⁷ A.T. Goshaw,¹⁵ K. Goulianatos,⁵⁰ A. Gresele,⁴³ M. Griffiths,²⁹ S. Grinstein,²¹ C. Grossi-Pilcher,¹³ R.C. Group,¹⁷ U. Grundler,²³ J. Guimaraes da Costa,²¹ Z. Gunay-Unalan,³⁵ C. Haber,²⁸ K. Hahn,³² S.R. Hahn,¹⁶ E. Halkiadakis,⁵² A. Hamilton,³³ B.-Y. Han,⁴⁹ J.Y. Han,⁴⁹ R. Handler,⁵⁹ F. Happacher,¹⁸ K. Hara,⁵⁵ M. Hare,⁵⁶ S. Harper,⁴² R.F. Harr,⁵⁸ R.M. Harris,¹⁶ M. Hartz,⁴⁷ K. Hatakeyama,⁵⁰ J. Hauser,⁸ A. Heijboer,⁴⁵ B. Heinemann,²⁹ J. Heinrich,⁴⁵ C. Henderson,³² M. Herndon,⁵⁹ J. Heuser,²⁵ D. Hidas,¹⁵ C.S. Hill,¹⁰ D. Hirschbuehl,²⁵ A. Hocker,¹⁶ A. Holloway,²¹ S. Hou,¹ M. Houlden,²⁹ S.-C. Hsu,⁹ B.T. Huffman,⁴² R.E. Hughes,³⁹ U. Husemann,⁶⁰ J. Huston,³⁵ J. Incandela,¹⁰ G. Introzzi,⁴⁶ M. Iori,⁵¹ Y. Ishizawa,⁵⁵ A. Ivanov,⁷ B. Iyutin,³² E. James,¹⁶ D. Jang,⁵² B. Jayatilaka,³⁴ D. Jeans,⁵¹ H. Jensen,¹⁶ E.J. Jeon,²⁷ S. Jindariani,¹⁷ M. Jones,⁴⁸ K.K. Joo,²⁷ S.Y. Jun,¹² J.E. Jung,²⁷ T.R. Junk,²³ T. Kamon,⁵³ P.E. Karchin,⁵⁸ Y. Kato,⁴¹ Y. Kemp,²⁵ R. Kephart,¹⁶ U. Kerzel,²⁵ V. Khotilovich,⁵³ B. Kilminster,³⁹ D.H. Kim,²⁷ H.S. Kim,²⁷ J.E. Kim,²⁷ M.J. Kim,¹² S.B. Kim,²⁷ S.H. Kim,⁵⁵ Y.K. Kim,¹³ N. Kimura,⁵⁵ L. Kirsch,⁶ S. Klimenko,¹⁷ M. Klute,³² B. Knuteson,³² B.R. Ko,¹⁵ K. Kondo,⁵⁷ D.J. Kong,²⁷ J. Konigsberg,¹⁷ A. Korytov,¹⁷ A.V. Kotwal,¹⁵ A. Kovalev,⁴⁵ A.C. Kraan,⁴⁵ J. Kraus,²³ I. Kravchenko,³² M. Kreps,²⁵ J. Kroll,⁴⁵ N. Krumnack,⁴ M. Kruse,¹⁵ V. Krutelyov,¹⁰ T. Kubo,⁵⁵ S. E. Kuhlmann,² T. Kuhr,²⁵ Y. Kusakabe,⁵⁷ S. Kwang,¹³ A.T. Laasanen,⁴⁸ S. Lai,³³ S. Lami,⁴⁶ S. Lammel,¹⁶ M. Lancaster,³⁰ R.L. Lander,⁷ K. Lannon,³⁹ A. Lath,⁵² G. Latino,⁴⁶ I. Lazzizzera,⁴³ T. LeCompte,² J. Lee,⁴⁹ J. Lee,²⁷ Y.J. Lee,²⁷ S.W. Lee,⁵³ R. Lefèvre,³ N. Leonardo,³² S. Leone,⁴⁶ S. Levy,¹³ J.D. Lewis,¹⁶ C. Lin,⁶⁰ C.S. Lin,¹⁶ M. Lindgren,¹⁶ E. Lipeles,⁹ T.M. Liss,²³ A. Lister,⁷ D.O. Litvintsev,¹⁶ T. Liu,¹⁶ N.S. Lockyer,⁴⁵ A. Loginov,³⁶ M. Loreti,⁴³ P. Loverre,⁵¹ R.-S. Lu,¹ D. Lucchesi,⁴³ P. Lujan,²⁸ P. Lukens,¹⁶ G. Lungu,¹⁷ L. Lyons,⁴² J. Lys,²⁸ R. Lysak,¹ E. Lytken,⁴⁸ P. Mack,²⁵ D. MacQueen,³³ R. Madrak,¹⁶ K. Maeshima,¹⁶ K. Makhoul,³² T. Maki,²² P. Maksimovic,²⁴ S. Malde,⁴² G. Manca,²⁹ F. Margaroli,⁵ R. Marginean,¹⁶ C. Marino,²⁵ C.P. Marino,²³ A. Martin,⁶⁰ M. Martin,²⁴ V. Martin,²⁰ M. Martínez,³ T. Maruyama,⁵⁵ P. Mastrandrea,⁵¹ T. Masubuchi,⁵⁵ H. Matsunaga,⁵⁵ M.E. Mattson,⁵⁸ R. Mazini,³³ P. Mazzanti,⁵ K.S. McFarland,⁴⁹ P. McIntyre,⁵³ R. McNulty,²⁹ A. Mehta,²⁹ P. Mehtala,²² S. Menzemer,¹¹ A. Menzione,⁴⁶ P. Merkel,⁴⁸ C. Mesropian,⁵⁰ A. Messina,⁵¹ T. Miao,¹⁶ N. Miladinovic,⁶ J. Miles,³² R. Miller,³⁵ C. Mills,¹⁰ M. Milnik,²⁵ A. Mitra,¹ G. Mitselmakher,¹⁷ A. Miyamoto,²⁶ S. Moed,¹⁹ N. Moggi,⁵ B. Mohr,⁸ R. Moore,¹⁶ M. Morello,⁴⁶ P. Movilla Fernandez,²⁸ J. Mühlstädt,²⁸ A. Mukherjee,¹⁶

Th. Muller,²⁵ R. Mumford,²⁴ P. Murat,¹⁶ J. Nachtman,¹⁶ A. Nagano,⁵⁵ J. Naganoma,⁵⁷ S. Nahn,³² I. Nakano,⁴⁰
 A. Napier,⁵⁶ V. Necula,¹⁷ C. Neu,⁴⁵ M.S. Neubauer,⁹ J. Nielsen,²⁸ T. Nigmanov,⁴⁷ L. Nodulman,² O. Norniella,³
 E. Nurse,³⁰ S.H. Oh,¹⁵ Y.D. Oh,²⁷ I. Oksuzian,¹⁷ T. Okusawa,⁴¹ R. Oldeman,²⁹ R. Orava,²² K. Osterberg,²²
 C. Pagliarone,⁴⁶ E. Palencia,¹¹ V. Papadimitriou,¹⁶ A.A. Paramonov,¹³ B. Parks,³⁹ S. Pashapour,³³ J. Patrick,¹⁶
 G. Pauleta,⁵⁴ M. Paulini,¹² C. Paus,³² D.E. Pellett,⁷ A. Penzo,⁵⁴ T.J. Phillips,¹⁵ G. Piacentino,⁴⁶ J. Piedra,⁴⁴
 L. Pinera,¹⁷ K. Pitts,²³ C. Plager,⁸ L. Pondrom,⁵⁹ X. Portell,³ O. Poukhov,¹⁴ N. Pounder,⁴² F. Prokoshin,¹⁴
 A. Pronko,¹⁶ J. Proudfoot,² F. Ptochos,¹⁸ G. Punzi,⁴⁶ J. Pursley,²⁴ J. Rademacker,⁴² A. Rahaman,⁴⁷ N. Ranjan,⁴⁸
 S. Rappoccio,²¹ B. Reisert,¹⁶ V. Rekovic,³⁷ P. Renton,⁴² M. Rescigno,⁵¹ S. Richter,²⁵ F. Rimondi,⁵ L. Ristori,⁴⁶
 A. Robson,²⁰ T. Rodrigo,¹¹ E. Rogers,²³ S. Rolli,⁵⁶ R. Roser,¹⁶ M. Rossi,⁵⁴ R. Rossin,¹⁷ A. Ruiz,¹¹ J. Russ,¹²
 V. Rusu,¹³ H. Saarikko,²² S. Sabik,³³ A. Safonov,⁵³ W.K. Sakumoto,⁴⁹ G. Salamanna,⁵¹ O. Saltó,³ D. Saltzberg,⁸
 C. Sánchez,³ L. Santi,⁵⁴ S. Sarkar,⁵¹ L. Sartori,⁴⁶ K. Sato,¹⁶ P. Savard,³³ A. Savoy-Navarro,⁴⁴ T. Scheidle,²⁵
 P. Schlabach,¹⁶ E.E. Schmidt,¹⁶ M.P. Schmidt,⁶⁰ M. Schmitt,³⁸ T. Schwarz,⁷ L. Scodellaro,¹¹ A.L. Scott,¹⁰
 A. Scribano,⁴⁶ F. Scuri,⁴⁶ A. Sedov,⁴⁸ S. Seidel,³⁷ Y. Seiya,⁴¹ A. Semenov,¹⁴ L. Sexton-Kennedy,¹⁶ A. Sfyrla,¹⁹
 M.D. Shapiro,²⁸ T. Shears,²⁹ P.F. Shepard,⁴⁷ D. Sherman,²¹ M. Shimojima,⁵⁵ M. Shochet,¹³ Y. Shon,⁵⁹
 I. Shreyber,³⁶ A. Sidoti,⁴⁶ P. Sinervo,³³ A. Sisakyan,¹⁴ J. Sjolin,⁴² A.J. Slaughter,¹⁶ J. Slaunwhite,³⁹ K. Sliwa,⁵⁶
 J.R. Smith,⁷ F.D. Snider,¹⁶ R. Snihur,³³ M. Soderberg,³⁴ A. Soha,⁷ S. Somalwar,⁵² V. Sorin,³⁵ J. Spalding,¹⁶
 F. Spinella,⁴⁶ T. Spreitzer,³³ P. Squillacioti,⁴⁶ M. Stanitzki,⁶⁰ A. Staveris-Polykalas,⁴⁶ R. St. Denis,²⁰ B. Stelzer,⁸
 O. Stelzer-Chilton,⁴² D. Stentz,³⁸ J. Strologas,³⁷ D. Stuart,¹⁰ J.S. Suh,²⁷ A. Sukhanov,¹⁷ H. Sun,⁵⁶ T. Suzuki,⁵⁵
 A. Taffard,²³ R. Takashima,⁴⁰ Y. Takeuchi,⁵⁵ K. Takikawa,⁵⁵ M. Tanaka,² R. Tanaka,⁴⁰ M. Tecchio,³⁴ P.K. Teng,¹
 K. Terashi,⁵⁰ R.J. Tesarek,¹⁶ J. Thom,¹⁶ A.S. Thompson,²⁰ E. Thomson,⁴⁵ P. Tipton,⁶⁰ V. Tiwari,¹² S. Tkaczyk,¹⁶
 D. Toback,⁵³ S. Tokar,¹⁴ K. Tollefson,³⁵ T. Tomura,⁵⁵ D. Tonelli,⁴⁶ S. Torre,¹⁸ D. Torretta,¹⁶ S. Tourneur,⁴⁴
 W. Trischuk,³³ R. Tsuchiya,⁵⁷ S. Tsuno,⁴⁰ N. Turini,⁴⁶ F. Ukegawa,⁵⁵ T. Unverhau,²⁰ S. Uozumi,⁵⁵ D. Usynin,⁴⁵
 S. Vallecorsa,¹⁹ N. van Remortel,²² A. Varganov,³⁴ E. Vataga,³⁷ F. Vázquez,¹⁷ G. Velev,¹⁶ G. Veramendi,²³
 (CDF Collaboration)

¹*Institute of Physics, Academia Sinica, Taipei, Taiwan 11529, Republic of China*

²*Argonne National Laboratory, Argonne, Illinois 60439*

³*Institut de Fisica d'Altes Energies, Universitat Autònoma de Barcelona, E-08193, Bellaterra (Barcelona), Spain*

⁴*Baylor University, Waco, Texas 76798*

⁵*Istituto Nazionale di Fisica Nucleare, University of Bologna, I-40127 Bologna, Italy*

⁶*Brandeis University, Waltham, Massachusetts 02254*

⁷*University of California, Davis, Davis, California 95616*

⁸*University of California, Los Angeles, Los Angeles, California 90024*

⁹*University of California, San Diego, La Jolla, California 92093*

¹⁰*University of California, Santa Barbara, Santa Barbara, California 93106*

¹¹*Instituto de Fisica de Cantabria, CSIC-University of Cantabria, 39005 Santander, Spain*

¹²*Carnegie Mellon University, Pittsburgh, PA 15213*

¹³*Enrico Fermi Institute, University of Chicago, Chicago, Illinois 60637*

¹⁴*Joint Institute for Nuclear Research, RU-141980 Dubna, Russia*

¹⁵*Duke University, Durham, North Carolina 27708*

¹⁶*Fermi National Accelerator Laboratory, Batavia, Illinois 60510*

¹⁷*University of Florida, Gainesville, Florida 32611*

¹⁸*Laboratori Nazionali di Frascati, Istituto Nazionale di Fisica Nucleare, I-00044 Frascati, Italy*

¹⁹*University of Geneva, CH-1211 Geneva 4, Switzerland*

²⁰*Glasgow University, Glasgow G12 8QQ, United Kingdom*

²¹*Harvard University, Cambridge, Massachusetts 02138*

²²*Division of High Energy Physics, Department of Physics, University of Helsinki and Helsinki Institute of Physics, FIN-00014, Helsinki, Finland*

²³*University of Illinois, Urbana, Illinois 61801*

²⁴*The Johns Hopkins University, Baltimore, Maryland 21218*

- ²⁵Institut für Experimentelle Kernphysik, Universität Karlsruhe, 76128 Karlsruhe, Germany
²⁶High Energy Accelerator Research Organization (KEK), Tsukuba, Ibaraki 305, Japan
²⁷Center for High Energy Physics: Kyungpook National University, Taegu 702-701, Korea; Seoul National University, Seoul 151-742, Korea; and SungKyunKwan University, Suwon 440-746, Korea
²⁸Ernest Orlando Lawrence Berkeley National Laboratory, Berkeley, California 94720
²⁹University of Liverpool, Liverpool L69 7ZE, United Kingdom
³⁰University College London, London WC1E 6BT, United Kingdom
³¹Centro de Investigaciones Energeticas Medioambientales y Tecnologicas, E-28040 Madrid, Spain
³²Massachusetts Institute of Technology, Cambridge, Massachusetts 02139
³³Institute of Particle Physics: McGill University, Montréal, Canada H3A 2T8; and University of Toronto, Toronto, Canada M5S 1A7
³⁴University of Michigan, Ann Arbor, Michigan 48109
³⁵Michigan State University, East Lansing, Michigan 48824
³⁶Institution for Theoretical and Experimental Physics, ITEP, Moscow 117259, Russia
³⁷University of New Mexico, Albuquerque, New Mexico 87131
³⁸Northwestern University, Evanston, Illinois 60208
³⁹The Ohio State University, Columbus, Ohio 43210
⁴⁰Okayama University, Okayama 700-8530, Japan
⁴¹Osaka City University, Osaka 588, Japan
⁴²University of Oxford, Oxford OX1 3RH, United Kingdom
⁴³University of Padova, Istituto Nazionale di Fisica Nucleare, Sezione di Padova-Trento, I-35131 Padova, Italy
⁴⁴LPNHE, Université Pierre et Marie Curie/IN2P3-CNRS, UMR7585, Paris, F-75252 France
⁴⁵University of Pennsylvania, Philadelphia, Pennsylvania 19104
⁴⁶Istituto Nazionale di Fisica Nucleare Pisa, Universities of Pisa, Siena and Scuola Normale Superiore, I-56127 Pisa, Italy
⁴⁷University of Pittsburgh, Pittsburgh, Pennsylvania 15260
⁴⁸Purdue University, West Lafayette, Indiana 47907
⁴⁹University of Rochester, Rochester, New York 14627
⁵⁰The Rockefeller University, New York, New York 10021
⁵¹Istituto Nazionale di Fisica Nucleare, Sezione di Roma 1, University of Rome "La Sapienza," I-00185 Roma, Italy
⁵²Rutgers University, Piscataway, New Jersey 08855
⁵³Texas A&M University, College Station, Texas 77843
⁵⁴Istituto Nazionale di Fisica Nucleare, University of Trieste/ Udine, Italy
⁵⁵University of Tsukuba, Tsukuba, Ibaraki 305, Japan
⁵⁶Tufts University, Medford, Massachusetts 02155
⁵⁷Waseda University, Tokyo 169, Japan
⁵⁸Wayne State University, Detroit, Michigan 48201
⁵⁹University of Wisconsin, Madison, Wisconsin 53706
⁶⁰Yale University, New Haven, Connecticut 06520

We report a measurement of the Λ_b^0 lifetime in the exclusive decay $\Lambda_b^0 \rightarrow J/\psi \Lambda^0$ in $p\bar{p}$ collisions at $\sqrt{s} = 1.96$ TeV using an integrated luminosity of 1.0 fb^{-1} of data collected by the CDF II detector at the Fermilab Tevatron. Using fully reconstructed decays, we measure $\tau(\Lambda_b^0) = 1.593^{+0.083}_{-0.078} \text{ (stat.)} \pm 0.033 \text{ (syst.) ps}$. This is the single most precise measurement of $\tau(\Lambda_b^0)$ and is 3.2σ higher than the current world average.

PACS numbers: 13.30.Eg 14.20.Mr

The weak decay of quarks depends on fundamental parameters of the standard model, including elements of the Cabibbo-Kobayashi-Maskawa (CKM) matrix which describe mixing between quark families. Extraction of these parameters from weak decays is complicated since observed quarks are not free but are confined within color-singlet hadrons, as described by quantum chromodynamics (QCD). An essential tool used in this extraction is the heavy quark expansion (HQE) technique [1, 2]. In HQE, the total decay width of a heavy hadron is expressed as an expansion in inverse powers of the heavy

quark mass m_q . Lifetime ratios of b -flavored hadrons are predicted to be unity through $O(1/m_b)$, and $O(1/m_b^2)$ corrections are small ($\lesssim 2\%$) [3]. Detailed analysis of $O(1/m_b^3)$ corrections to the lifetime ratio lead to an expected value of $\frac{\tau(\Lambda_b^0)}{\tau(B^0)} \simeq 0.94$ [4]. This theoretical prediction has been in poor agreement with measurements for more than a decade [5–9]. The current world average of the Λ_b^0 lifetime is $1.230 \pm 0.074 \text{ ps}$, corresponding to a ratio of $\frac{\tau(\Lambda_b^0)}{\tau(B^0)} = 0.804 \pm 0.049$ [10]. Recent calculations including next-to-leading-order QCD and $O(1/m_b^4)$

corrections lower the prediction [11, 12], making it more consistent with the measurements.

In this Letter, we present a measurement of the Λ_b^0 lifetime, $\tau(\Lambda_b^0)$, in the fully reconstructed decay $\Lambda_b^0 \rightarrow J/\psi \Lambda^0$, with $J/\psi \rightarrow \mu^+ \mu^-$ and $\Lambda^0 \rightarrow p\pi^-$. Charge conjugate modes are implied throughout. Our data sample consists of 1.0 fb^{-1} of $p\bar{p}$ collisions at $\sqrt{s} = 1.96 \text{ TeV}$ collected by the CDF II detector at the Fermilab Tevatron between February 2002 and February 2006. This is the first measurement of $\tau(\Lambda_b^0)$ using fully reconstructed decays that is competitive with the best previous measurements, which are based on semileptonic decays. As compared to fully reconstructed decays, measurements using partially reconstructed semileptonic decays have additional uncertainties due to the missing energy of the unobserved neutrino and the modeling of background from other b -flavored baryons.

As a check of our method, we also measure $\tau(B^0)$ using a sample of $B^0 \rightarrow J/\psi K_S^0$ decays, which has larger yield than the Λ_b^0 sample. This decay channel is topologically similar to $\Lambda_b^0 \rightarrow J/\psi \Lambda^0$, since both K_S^0 and Λ^0 decay with large displacement from the b -hadron-decay vertex. The analysis procedure for Λ_b^0 is developed using $B^0 \rightarrow J/\psi K_S^0$ only and checked using other b -meson decays containing a $J/\psi \rightarrow \mu^+ \mu^-$ in the final state. The Λ_b^0 lifetime was not extracted until all procedures were established including the estimate of the systematic uncertainty.

The components of the CDF II detector relevant to this analysis are described briefly here; a more complete description can be found elsewhere [13]. Charged particles are reconstructed using an open-cell drift chamber called the central outer tracker (COT) [14] and 7 layers of silicon microstrip detectors with radii between 2.4 cm and 28 cm [15]. These are immersed in a 1.4 T solenoidal magnetic field and cover the range $|\eta| \leq 1$, where η is the pseudorapidity defined as $\eta \equiv -\ln \tan(\theta/2)$ and θ is the polar angle [16]. Four layers of planar drift chambers (CMU) [17] detect muons with transverse momentum $p_T > 1.4 \text{ GeV}/c$ within $|\eta| < 0.6$. Additional chambers and scintillators (CMX) [18] cover $0.6 < |\eta| < 1.0$ for muons with $p_T > 2.0 \text{ GeV}/c$.

A sample of $J/\psi \rightarrow \mu^+ \mu^-$ candidates, collected using a dimuon trigger, is selected to begin the reconstruction of Λ_b^0 and B^0 candidates. At level 1 of a three-level trigger system, the eXtremely Fast Tracker (XFT) [19] uses COT information to fit tracks. Those tracks with $p_T > 1.5(2.0) \text{ GeV}/c$ are extrapolated to the CMU (CMX) chambers and compared with the positions of muon-chamber tracks. The event passes level 1 if two or more XFT tracks are matched to muon-chamber tracks. Opposite-charge and opening-angle requirements are imposed at level 2. At level 3, full tracking information is used to reconstruct $J/\psi \rightarrow \mu^+ \mu^-$ candidates. Events with a candidate in the mass range 2.7 to $4.0 \text{ GeV}/c^2$ are accepted at level 3 and permanently recorded for further

analysis.

Tracks from two triggered muons are constrained to originate from a common vertex to make a $J/\psi \rightarrow \mu^+ \mu^-$ candidate. To ensure a high-quality vertex for the lifetime measurement, each muon track is required to have at least 3 axial hits in the silicon system. The reconstructed $\mu^+ \mu^-$ invariant mass is required to be in the range $3.014 < M_{\mu^+ \mu^-} < 3.174 \text{ GeV}/c^2$. This corresponds to approximately $\pm 4\sigma$ of the reconstructed width, which is dominated by the resolution [20].

We construct $K_S^0 \rightarrow \pi^+ \pi^-$ and $\Lambda^0 \rightarrow p\pi^-$ candidates from pairs of oppositely-charged tracks fit to a common vertex. Since many K_S^0 and Λ^0 decays occur outside some layers of the silicon system due to their long lifetime, their tracks are not required to have silicon hits. We suppress K_S^0 and Λ^0 cross contamination by rejecting K_S^0 (Λ^0) candidates with proton-pion (dipion) invariant mass in the range [1.1085, 1.1235] ([0.48175, 0.5115]) GeV/c^2 .

The B^0 and Λ_b^0 candidates are reconstructed by associating J/ψ candidates with K_S^0 or Λ^0 candidates in each event. We choose further selection requirements for our b -hadron samples that optimize $S/\sqrt{S+B}$ where S and B are the numbers of signal and background events, respectively. In the optimization procedure, S is estimated using a Monte Carlo simulation, while B is estimated using the b -hadron invariant mass sidebands, which are chosen to exclude the data used in the lifetime fits to avoid any potential bias.

The selection requirements resulting from the optimization are described below. We require $0.473 < M_{\pi\pi} < 0.523 \text{ GeV}/c^2$ and $p_T > 1.5 \text{ GeV}/c$ for K_S^0 candidates. For Λ^0 candidates, we require $1.107 < M_{p\pi} < 1.125 \text{ GeV}/c^2$ and $p_T > 2.6 \text{ GeV}/c$. We require $L_{xy}^{V^0}/\sigma_{L_{xy}^{V^0}} > 6$ for K_S^0 and $L_{xy}^{V^0}/\sigma_{L_{xy}^{V^0}} > 4$ for Λ^0 , where $L_{xy}^{V^0}$ is defined as the distance from the J/ψ vertex to the $V^0 (\equiv K_S^0, \Lambda^0)$ vertex projected onto the V^0 transverse momentum vector and $\sigma_{L_{xy}^{V^0}}$ is its estimated uncertainty. Both B^0 and Λ_b^0 candidates are required to have $p_T > 4.0 \text{ GeV}/c$. Finally, the χ^2 of a b -hadron kinematic fit is required to be less than 26 for 5 degrees of freedom. This fit finds the best b -hadron decay vertex and momentum subject to the constraints that the muon tracks originate from a common vertex, the K_S^0 or Λ^0 tracks originate from a common vertex with combined momentum pointing back in three dimensions to the dimuon vertex, and the invariant mass of the two muons is equal to the world average J/ψ mass [10]. The invariant mass distributions of the B^0 and Λ_b^0 candidates passing these requirements are shown in Fig. 1. The yields are $N(B^0 \rightarrow J/\psi K_S^0) = 3376 \pm 88$ (stat.) and $N(\Lambda_b^0 \rightarrow J/\psi \Lambda^0) = 538 \pm 38$ (stat.).

The lifetime of a B^0 and Λ_b^0 is determined from the distribution of proper decay time t given by $ct \equiv L_{xy}^b / (\beta\gamma)_T^b = L_{xy}^b c M_b / p_T^b$, where L_{xy}^b is the distance traveled by each b -hadron candidate along the direction

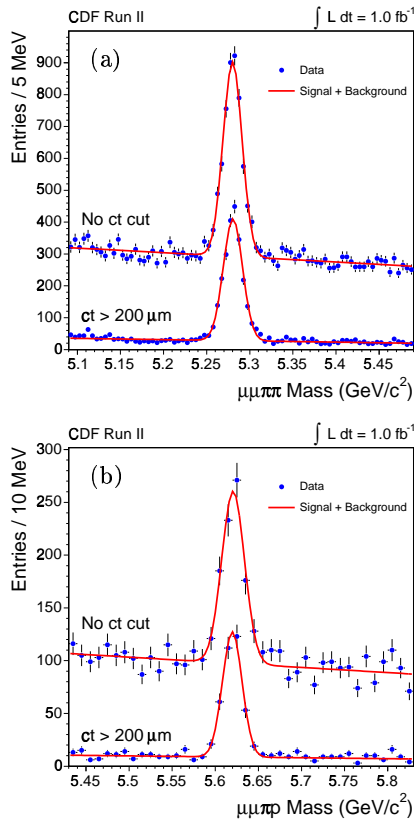


FIG. 1: Invariant mass distribution of (a) $B^0 \rightarrow J/\psi K_S^0$ and (b) $\Lambda_b^0 \rightarrow J/\psi \Lambda_b^0$ candidates. The distributions with $ct > 200 \mu\text{m}$, where t is the proper decay time, illustrate that the majority of backgrounds originate from the primary interaction vertex. The distributions are fit to the sum of a Gaussian signal and linear background.

of its transverse momentum p_T^b and $(\beta\gamma)_T^b \equiv p_T^b/(cM_b)$ is the transverse boost, where M_b is the world average mass of the b hadron [10]. Since the J/ψ vertex occurs at the same point as the b hadron decay and is well determined, it is used as the b -hadron decay vertex. The b hadron is assumed to originate from the average beamline determined on a run-by-run basis using inclusive jet data. The primary vertex for a given event is the $x - y$ position of this beamline at the average z coordinate of the muon tracks at their closest approach to the beamline.

The lifetimes are extracted using the maximum likelihood method. The likelihood function \mathcal{L} is multivariate, and is constructed from the products of single variable probability density functions describing the distributions of the invariant mass m_i , ct_i , and their respective estimated resolutions σ_i^m and σ_i^{ct} . It is given by

$$\begin{aligned} \mathcal{L} = \prod_{i=1}^N & \left[(1 - f_B) \mathcal{P}_S^{ct}(ct_i|\sigma_i^{ct}) \mathcal{P}_S^{\sigma^{ct}}(\sigma_i^{ct}) \mathcal{P}_S^m(m_i|\sigma_i^m) \right. \\ & \left. + f_B \mathcal{P}_B^{ct}(ct_i|\sigma_i^{ct}) \mathcal{P}_B^{\sigma^{ct}}(\sigma_i^{ct}) \mathcal{P}_B^m(m_i|\sigma_i^m) \right], \end{aligned}$$

where N is the number of events in the b -hadron mass window, f_B is the background fraction, and \mathcal{P}^{ct} , $\mathcal{P}^{\sigma^{ct}}$, and \mathcal{P}^m are probability density functions for ct , σ^{ct} , and mass, respectively. The mass resolution probability distributions $\mathcal{P}^{\sigma^m}(\sigma_i^m)$ do not appear in \mathcal{L} because they are equal for signal and background, within the available statistics. Since this is not true for the ct resolution distributions, $\mathcal{P}^{\sigma^{ct}}$ must be included in \mathcal{L} [21].

The mass distribution is modeled as the sum of a Gaussian signal and linear background, where the Gaussian width σ_i^m is scaled by a parameter to account for misestimation of the mass resolutions. The ct distribution is modeled by the sum of five components, all convoluted with a Gaussian resolution function with a scale factor parameter for the σ_i^{ct} : a positive exponential ($e^{-ct_i/\tau}/\tau$) for the signal, a δ -function representing the zero-lifetime component, one negative and two positive exponentials accounting for mismeasured decay vertices and background from other heavy-flavor decays. The relative contribution of each of the background components is determined by the fit. The σ^{ct} distribution is modeled by a Gaussian convoluted with an exponential for both signal and background.

We fit over the mass range [5.170, 5.390] and [5.521, 5.721] GeV/c^2 for B^0 and Λ_b^0 , respectively. These ranges provide a sufficient sideband to constrain the background shape while avoiding regions where the mass distribution has complex structure. For both B^0 and Λ_b^0 , we require $\sigma_i^m < 20 \text{ MeV}/c^2$ and fit over the range [-2000, 4000] μm in ct and [0, 100] μm in σ^{ct} . We maximize the likelihood to determine the best values of all fit model parameters, including the signal lifetimes $\tau(B^0) = 456.8^{+9.0}_{-8.9} \mu\text{m}$ and $\tau(\Lambda_b^0) = 477.6^{+25.0}_{-23.4} \mu\text{m}$. Fit projections are shown in Fig. 2.

Systematic uncertainties come from four main sources: fitting procedure and model, primary vertex determination, alignment of detector elements, and K_S^0 or Λ^0 pointing requirement in the B^0 or Λ_b^0 kinematic fit. The fitting bias is determined using a simple Monte Carlo simulation in which events are distributed according to the fit model. The bias was found to be less than $0.4 \mu\text{m}$ and $0.5 \mu\text{m}$ for B^0 and Λ_b^0 , respectively. The systematic uncertainties due to ct resolution and mass resolution are estimated by including additional Gaussian components to their respective parts of the model in separate fits to the data and observing the deviations from the nominal result. We estimate the contribution from our mass background model by fitting with a uniform rather than linear background shape. The systematic uncertainty due to the ct background model is estimated by fitting with two or four background exponentials convoluted with the resolution function and fitting with two, three, or four background exponentials without convolution. We study a possible mass dependence in the ct background shape by separately fitting for B^0 (Λ_b^0) lifetime in the following low and high mass regions: [5.170, 5.3225] ([5.521, 5.651])

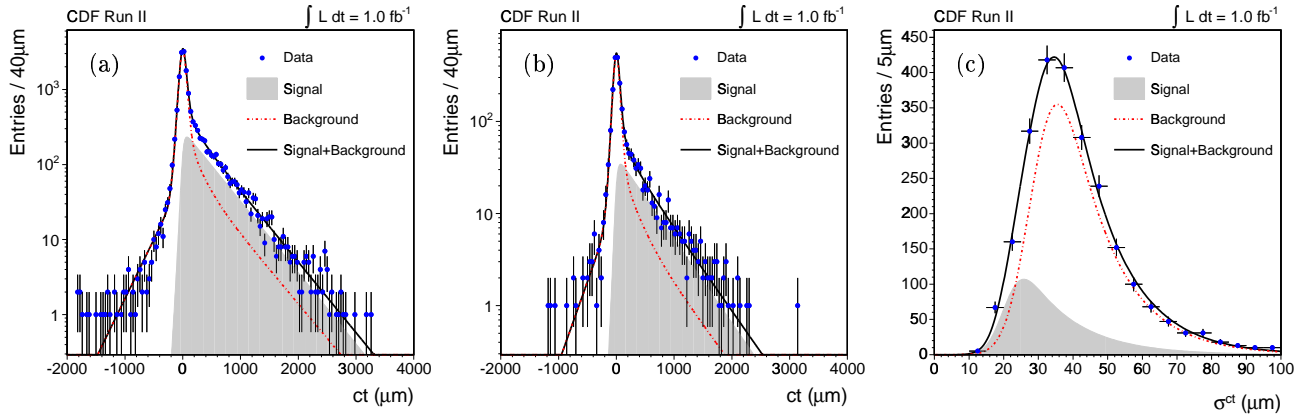


FIG. 2: (a) ct fit projection for $B^0 \rightarrow J/\psi K_S^0$ candidates; and (b) ct and (c) σ^{ct} fit projections for $\Lambda_b^0 \rightarrow J/\psi \Lambda^0$ candidates.

and [5.2375, 5.390] ([5.591, 5.721]) GeV/c^2 . The observed shifts are consistent with the statistical differences of the two samples for both modes. We use the average shift of $1.9 \mu\text{m}$ and $4.1 \mu\text{m}$ for B^0 and Λ_b^0 , respectively, as an estimate of the systematic uncertainty due to a mass-dependent ct background. We estimate the systematic uncertainty due to our σ^{ct} and σ^m distribution models by the observed shift between simple Monte Carlo events generated with the data distributions but fit with our model compared with simple Monte Carlo events both generated and fit with our model. Using the same simple Monte Carlo technique, we estimate the systematic uncertainty due to a correlation between the ct and σ^{ct} for the background component by generating simple Monte Carlo data sets with the correlation observed in the data and fitting with our baseline model where this correlation is absent.

We estimate the systematic uncertainty due to our primary vertex determination by comparing different choices of the z coordinate used to evaluate the run-averaged beamline. We estimate uncertainties due to any residual misalignments of the silicon detector using Monte Carlo samples generated with radial displacements of individual sensors (internal alignment) and relative translation and rotation of the silicon detector with respect to the COT (global alignment). We also study the resolution and bias on the V^0 pointing to the J/ψ vertex in data. If these were strongly ct -dependent, the kinematic fit quality requirement could bias the b -hadron lifetime. We observe no lifetime bias and assign uncertainties of $0.6 \mu\text{m}$ for B^0 and $5.4 \mu\text{m}$ for Λ_b^0 based on the statistical precision of our study.

The systematic uncertainties are summarized in Table I. We obtain total systematic uncertainties of $4.9 \mu\text{m}$ for B^0 and $9.9 \mu\text{m}$ for Λ_b^0 by adding the individual uncertainties in quadrature.

A number of cross checks on the analysis procedure are performed. We measure the B^+ and B^0 lifetimes which are statistically consistent with the world aver-

TABLE I: Systematic uncertainties (in μm) for the measurement of $c\tau(B^0)$ and $c\tau(\Lambda_b^0)$. The total uncertainties are the individual uncertainties added in quadrature.

Source	$c\tau(B^0)$	$c\tau(\Lambda_b^0)$
Fitter Bias	0.4	0.5
Fit Model:		
ct Resolution	3.1	5.5
Mass Signal	0.7	2.3
Mass Background	0.1	0.1
ct Background	0.5	0.7
σ^{ct} Distribution Modeling	0.1	0.2
σ^m Distribution Modeling	0.6	0.2
Mass- ct Background Correlation	1.9	4.1
ct - σ^{ct} Background Correlation	0.3	1.3
Primary Vertex Determination	0.2	0.3
Alignment		
SVX Internal	2.0	2.0
SVX/COT Global	2.2	3.2
V^0 Pointing	0.6	5.4
Total	4.9	9.9

age values in the following decay modes: $B^0 \rightarrow \psi^{(i)} K_S^0$, $B^0 \rightarrow \psi^{(i)} K^{*0} (K^{*0} \rightarrow K^+ \pi^-)$, $B^+ \rightarrow \psi^{(i)} K^+$, and $B^+ \rightarrow \psi K^{*+} (K^{*+} \rightarrow K_S^0 \pi^+)$, with $\psi^{(i)} \rightarrow \mu^+ \mu^-$ and $\psi' \rightarrow \psi^+ \pi^-$. We search for unexpected lifetime dependence on the V^0 and b -hadron kinematics, data-taking period, number of tracks in the event, and use of silicon hits on V^0 daughter and muon tracks; no dependence is observed. Finally, we determine the lifetime using two alternative techniques which give results consistent with our baseline fit: a ct -only binned fit applied to sideband-subtracted data and a fit to the mass distribution in ct bins which is insensitive to details of the ct background shape.

In summary, we measure

$$\tau(\Lambda_b^0) = 1.593^{+0.083}_{-0.078} \text{ (stat.)} \pm 0.033 \text{ (syst.) ps.}$$

As a cross check, we also measure $\tau(B^0) = 1.524 \pm 0.030 \text{ (stat.)} \pm 0.016 \text{ (syst.) ps}$ which is consistent with

the world average $\tau(B^0) = 1.530 \pm 0.009$ ps. Our measurement of $\tau(\Lambda_b^0)$ is consistent with the DØ result in the same channel [7] at the 1.7σ level and is the first measurement using a fully reconstructed mode that reaches a precision comparable with the previous best measurements based on semileptonic decays of the Λ_b^0 . It is also comparable in precision to the current world average, but is 3.2σ higher [10]. Forming a ratio with the world average B^0 lifetime, we determine

$$\frac{\tau(\Lambda_b^0)}{\tau(B^0)} = 1.041 \pm 0.057 \text{ (stat. + syst.)}.$$

This ratio is consistent with the higher end of the theory predictions [4, 11, 12].

We thank the Fermilab staff and the technical staffs of the participating institutions for their vital contributions. This work was supported by the U.S. Department of Energy and National Science Foundation; the Italian Istituto Nazionale di Fisica Nucleare; the Ministry of Education, Culture, Sports, Science and Technology of Japan; the Natural Sciences and Engineering Research Council of Canada; the National Science Council of the Republic of China; the Swiss National Science Foundation; the A.P. Sloan Foundation; the Bundesministerium für Bildung und Forschung, Germany; the Korean Science and Engineering Foundation and the Korean Research Foundation; the Particle Physics and Astronomy Research Council and the Royal Society, UK; the Institut National de Physique Nucléaire et Physique des Particules/CNRS; the Russian Foundation for Basic Research; the Comisión Interministerial de Ciencia y Tecnología, Spain; the European Community's Human Potential Programme under contract HPRN-CT-2002-00292; and the Academy of Finland.

-
- [1] I. I. Y. Bigi, M. A. Shifman, and N. Uraltsev, Ann. Rev. Nucl. Part. Sci. **47**, 591 (1997).
 - [2] A. V. Manohar and M. B. Wise, Camb. Monogr. Part. Phys. Nucl. Phys. Cosmol. **10**, 1 (2000).
 - [3] I. I. Y. Bigi, N. G. Uraltsev, and A. I. Vainshtein, Phys. Lett. B **293**, 430 (1992).
 - [4] N. G. Uraltsev, Phys. Lett. B **376**, 303 (1996).
 - [5] R. Barate *et al.* (ALEPH Collaboration), Eur. Phys. J. C **2**, 197 (1998).
 - [6] F. Abe *et al.* (CDF Collaboration), Phys. Rev. Lett. **77**, 1439 (1996).
 - [7] V. M. Abazov *et al.* (DØ Collaboration), Phys. Rev. Lett. **94**, 102001 (2005).
 - [8] P. Abreu *et al.* (DELPHI Collaboration), Eur. Phys. J. C **10**, 185 (1999).
 - [9] K. Ackerstaff *et al.* (OPAL Collaboration), Phys. Lett. B **426**, 161 (1998).
 - [10] W. M. Yao *et al.* (Particle Data Group), J. Phys. G **33**, 1 (2006).
 - [11] F. Gabbiani, A. I. Onishchenko, and A. A. Petrov, Phys. Rev. D **70**, 094031 (2004).
 - [12] E. Franco, V. Lubicz, F. Mescia, and C. Tarantino, Nucl. Phys. B **633**, 212 (2002).
 - [13] R. Blair, *et al.* (CDF Collaboration) (1996), FERMILAB-PUB-96/390-E.
 - [14] T. Affolder *et al.*, Nucl. Instrum. Methods A **526**, 249 (2004).
 - [15] A. Sill *et al.*, Nucl. Instrum. Methods A **447**, 1 (2000).
 - [16] CDF II uses a cylindrical coordinate system in which φ is the azimuthal angle, r is the radius from the nominal beamline, and z points in the proton beam direction with the origin at the center of the detector. The transverse plane is the plane perpendicular to the z axis.
 - [17] G. Ascoli *et al.*, Nucl. Instrum. Methods A **268**, 33 (1988).
 - [18] T. Dorigo *et al.*, Nucl. Instrum. Methods A **461**, 560 (2001).
 - [19] E. J. Thomson *et al.*, IEEE Trans. Nucl. Sci. **49**, 1063 (2003).
 - [20] D. Acosta *et al.* (CDF Collaboration), Phys. Rev. D **71**, 032001 (2005).
 - [21] G. Punzi, eConf **C030908**, WELT002 (2003), arXiv:physics/0401045.